Final Draft
of the original manuscript:

Anisimova, N.; Kiselevskiy, M.; Martynenko, N.; Straumal, B.; Willumeit-Römer, R.; Dobatkin, S.; Estrin, Y.:

Cytotoxicity of biodegradable magnesium alloy WE43 to tumor cells in vitro: Bioresorbable implants with antitumor activity?

In: Journal of Biomedical Materials Research B. Vol. 108 (2020) 1, 167 - 173.
First published online by Wiley: 08.04.2019

https://dx.doi.org/10.1002/jbm.b.34375

Cytotoxicity of biodegradable magnesium alloy WE43 to tumor cells in vitro: Bioresorbable implants with antitumor activity?

Natalia Anisimova,[1,2] Mikhail Kiselevskiy,[1,2] Natalia Martynenko,[1,3] Boris Straumal,[1,4] Regine Willumeit-Römer,[5] Sergey Dobatkin,[1,3] Yuri Estrin[6,7]
[1]National University of Science and Technology "MISIS", Moscow, Russia
[2]N. N. Blokhin National Medical Research Center of Oncology, Ministry of Health of the Russian Federation, Moscow, Russia
[3]A.A. Baikov Institute of Metallurgy and Materials Science of the RAS, Moscow, Russia
[4]Institute of Solid State Physics, Russian Academy of Sciences, Chernogolovka, Russia
[5]Institute of Materials Research, Division Metallic Biomaterials, Helmholtz-Zentrum Geesthacht, Geesthacht, Germany
[6]Department of Materials Science and Engineering, Monash University, Melbourne, Australia
[7]Department of Mechanical Engineering, The University of Western Australia, Nedlands, Australia

Abstract

In this study, a degradable magnesium alloy WE43 (Mg–3.56%Y–2.20%Nd–0.47%Zr) was used as a research object. To refine its microstructure from the initial homogenized one, the alloy was subjected to severe plastic deformation (SPD) by equal channel angular pressing (ECAP). The data presented show that coincubation of tumor LNCaP and MDAMB- 231 cells with the WE43 alloy in the homogenized and the ECAP-processed states led to a decrease in their viability and proliferation. An increase in the concentration of Annexin V(+) cells during coincubation with samples in both microstructural states investigated was also observed. This is associated with the induction of apoptosis in the cell culture through contact with the samples. Concurrently, a significant drop in the concentration of Bcl-2(+) cells occurred. It was established that ECAP led to an enhancement of the cytotoxic activity of the alloy against tumor cells. This study demonstrated that alloy WE43 can be considered as a promising candidate for application in orthopedic implants in clinical oncology, where it could play a double role of a mechanically stable, yet bioresorbable, scaffold with local antitumor activity.

INTRODUCTION

The necessity for bone defect restoration after resection of primary and metastatic bone tumors requires the use of implants and fasteners from biocompatible materials that have mechanical properties similar to those of bone tissue. Currently, magnesium-based alloys are considered as a promising choice due to a combination of biocompatibility, good mechanical properties, and ability of bioresorption they possess. In addition, there are indications that for the right alloy composition, microstructure and degradation rate (DR) anti-inflammatory and to some extent antibacterial activities can be induced. Furthermore, some antitumor effect of Mg alloys was reported.[1-6] In this light, developing mechanically strong Mg-based implant materials exhibiting at the same time antitumor activity is extremely relevant for clinical oncology.

According to the results of Chen et al.,[7] the antitumor activity of magnesium is mediated by its ability to release hydrogen during biodegradation, which exerts a cytopathogenic effect on tumor cells. The study demonstrated cytotoxic activity of magnesium on rat mammary tumor cells *in vitro* and retardation of tumor growth in mice *in vivo*. Recent reports suggest that various alloying elements can enhance the cytotoxic properties of magnesium. Wu and coauthors[8] studied the cytotoxic effect of alloy Mg–Ca–Sr–Zn on the osteogenic sarcoma cell line U2OS. It was shown that Mg–1Ca–0.5Sr–*x*Zn (x = 0, 2, 4, 6 mass %) alloys inhibit the proliferation, viability, cell cycle, migration, and invasion of U2OS cells. The effect was associated with Zn ions released into the culture medium during biocorrosion, which impede the proliferation of tumor cells by changing the cell cycle and inducing cell apoptosis,[9-11] mediated changes in the mitochondrial membrane potential, and activation of the caspase cell cycle.[12] In addition, the ability of these tumor cells to migrate into the tissue is diminished through the inhibition of mitogen-activated protein kinase (MAPK) activation. However, U2OS cells are much more sensitive to the concentration of Mg than primary cells and they die of osmotic shock, which is quite common for such cell lines.[13]

Doping of magnesium alloys with rare-earth (RE) elements can stimulate their biological activity and, specifically, boost their antitumor effect. For example, Hakimi et al.[14] reported that the products of biocorrosion of an extruded Mg–Nd–Y–Zr alloy had a cytotoxic effect on mouse osteosarcoma cells *in vitro*—combined with a reduction of cell viability over 24–48 h after direct contact.

Arguably the most studied magnesium alloy for medical purposes is the commercial alloy WE43 (Mg–Y–(Nd + RE)–Zr). This alloy was the basis for successful development of approved implants for osteosynthesis.[15, 16] Moreover, the presence of RE elements in its composition gives reasons to believe it should exhibit antitumor activity. It is therefore of interest to study the ability of alloy WE43 to inhibit the growth and development of tumor cells when they are in contact with a metal implant. While the beneficial effect of equal channel angular pressing (ECAP) on the mechanical property profile of Mg alloys owing to grain refinement and favorable texture is well known, [17-19] the anticipated possibility of using ECAP-processed WE43 as a scaffold (an implant or a fixed device) for therapy of cancer patients looked like a very exciting possibility, which motivated this research. We thus investigated the antitumor activity of WE43 alloy both in the homogenized condition and after processing by ECAP.

MATERIALS AND METHODS

The object of research was magnesium alloy WE43 (Mg–3.56%Y–2.20%Nd–0.47%Zr). In the initial state, the alloy was homogenized at 525°C for 8 h. Billets machined from the alloy were then processed by ECAP with a stepwise decrease in the processing temperature from 425 to 300°C in 25°C decrements. Route Bc ECAP with a 120° die angle was used. At each temperature level, two passes were conducted. Details of the ECAP process are given in ref 19. Processing by ECAP led to a remarkable refinement of the microstructure, the initial grain size of 70 μm dropping by a factor of 100, and a concomitant improvement of the mechanical properties of the alloy.19

For cytological studies, samples in the form of a quarter of a disk with a radius of 4.6 ± 0.12 mm and thickness of 1.42 ± 0.04 mm were cut. Before testing, all samples were sterilized in 70% ethanol overnight and rinsed with a 0.9% NaCl solution. They were then immersed in RPMI-1640 medium (PanEco, Russia) and incubated at 37 °C in a humidified atmosphere of 5% CO_2 for 24 h. To evaluate the *in vitro* antitumor properties of alloy WE43 in both microstructural conditions, two representative cell lines were chosen: (1) LNCaP—human prostate carcinoma cell line (ATCC CRL-1740) and (2) MDA-MB-231—human breast adenocarcinoma cell line (ATCC HTB-26). Tumor cells were seeded on the samples placed in wells of a 24-well plate and co-incubated with the samples for 3 days in 2-mL RPMI-1640 supplemented with 10% fetal bovine serum (FBS, HyClon, UK), 1% penicillin–streptomycin and 2-mM L-glutamine (all supplied by PanEco, Russia) in a humidified atmosphere with 5% CO_2 at 37 °C. As a control, cell cultures incubated in wells not containing WE43 samples were used. The initial density of the seeded cells was 7.8×10^4 cells/mL in the case of LNCaP and 4×10^4 cells/mL in the case of MDA-MB-231. The growth medium was changed daily. At each of the designated points in time (Days 1, 2, and 3 after start of the coincubation), cell proliferation was evaluated by standard 3-(4,5-dimethylthiazol-2-yl)-2,5-diphenyltetrazolium bromide (MTT) assays after removing the cultivation medium. Culture medium of 600 μL contained 45 μL of MTT (Sigma-Aldrich Co.) in phosphate-buffered saline (PBS) solution (5 mg/mL). The solution was added in to each well, followed by continuous incubation for 4 h at 37 °C. After the culture medium was removed, the formazan reaction products were dissolved in 350-μL sodium dodecyl sulphate (Sigma-Aldrich Co.) overnight. The absorbance values were measured in 96-well plates using a multiwell plate reader LabSystem Multiscan MS (Thermo Fisher Scientific) at 540 versus 690 nm. Each experiment of MTT test was evaluated in triplicate. For viability, apoptosis, oxidative stress, and Bcl-2 analysis, the adherent cells were trypsinized and washed with PBS. Subsequently, the cells were subjected to staining using Muse Count @ Viability Kit, Muse Oxidative Stress Kit, Muse Bcl-2 Activation Dual detection Kit (all—MD Millipore Corporation, Billerica), and Annexin V Apoptosis Detection Kit (Novus Biological) following the manufacturers' protocols. The results were evaluated on a Muse Millipore Cell Analyzer (Merck KGaA, Darmstadt, Germany) and a BD Canto II cytometer (Becton Dickinson, San Jose) using the BD FACSDiva Software. To study oxidative stress, the concentration of cells with a high content of reactive oxygen radicals (ROS—reactive oxygen species [ROS], ROS(+) cells) was evaluated. Apoptotic cells were detected with Annexin V: Annexin V(+)PI(−) for early and Annexin V(+)PI(+) for late apoptosis. To study the Bcl-2 level, the concentration of cells with a high content of the peptide Bcl-2 (+) cells was evaluated. These experiments were evaluated in duplicate or triplicate at each of the designated times. The data were presented as a mean ± standard deviation (mean ± SD). Statistical evaluation was performed by one-way ANOVA analysis with the Statistica 6.0 software. A p-value <0.05 was considered to represent a statistically significant difference.

Out of a total of 27 samples prepared for biocompatibility tests for each of the two microstructural states of the alloy (initial homogenized and ECAP-processed ones), six specimens were used for each of the following four types of measurements: viability, proliferation, apoptosis, and oxidative stress testing. For the measurements of the Bcl-2 levels, three specimens per microstructural state were used.

The DR of the alloys was determined by weight loss measurements. In these degradation tests, nine specimens were tested for each microstructural state of the alloy. Every specimen was co-incubated with LNCaP cells in 2-mL RPMI-1640 supplemented with 10% FBS, 1% penicillin–streptomycin, and 2 mM L-glutamine (8×10^4 cells/mL) for 3 days in a humidified atmosphere with 5% CO_2 at 37°C. The medium was changed daily. After the immersion time, the samples were cleaned with a cleaning solution [a mixture of Cr_2O_3, $AgNO_3$, and $Ba(NO_3)_2$] and reagent water for 1 min (according to the ASTM_G1-03-E procedure) to remove the corrosion products and dried at room temperature. Then the weight loss was determined and the DR (in mm/year), was calculated according to the following equation (ASTM_G1-03-E code):

$$DR = 8.76 \times 10^4 \frac{W}{A \times T \times D}$$

Here W is the mass loss in grams, T is the time of exposure in hours, A is the sample surface area in cm^2, and D is the density of the alloy in g/cm^3.

RESULTS

Cell viability

The presented data show that the WE43 alloy in both homogenized and ECAP-processed condition induced a decrease in the viability of LNCaP and MDA-MB-231 tumor cells (Fig. 1). A statistically significant cytotoxic effect was observed on the second day (LNCaP cells) and the third day (MDA-MB-231 cells) of cultivation. In the ECAP-processed state, WE43 exhibited a more pronounced cytotoxic activity than in the homogenized state ($*p < 0.05$). The drop in LNCaP cells viability with respect to control was 21 ± 1.9% after the second day ($*p = 0.002$) and 18 ± 2% ($*p = 0.002$) after the third day. The viability MDA-MB-231 cells after 3 days of cultivation with as-received homogenized and ECAP-treated WE43 samples dropped by 21 ± 4.7% ($*p = 0.027$) and 31 ± 6.2% compared to control ($*p = 0.018$), respectively.

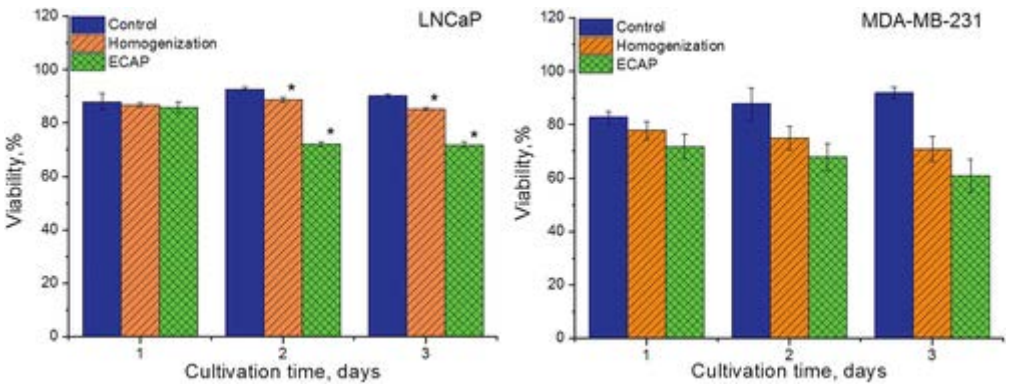

Figure 1
Effect of alloy WE43 in the homogenized and ECAP-treated states on the viability of LNCaP and MDA-MB-231 tumor cells (presented as a mean ± SD).

Cell proliferation assay

Significant inhibition of LNCaP cells proliferation was observed on the third day of coincubation with WE43 samples: the count of the live cells fell by a factor of 3.2 and 3.9 for the homogenized and ECAP-processed conditions versus control, respectively (Fig. 2).

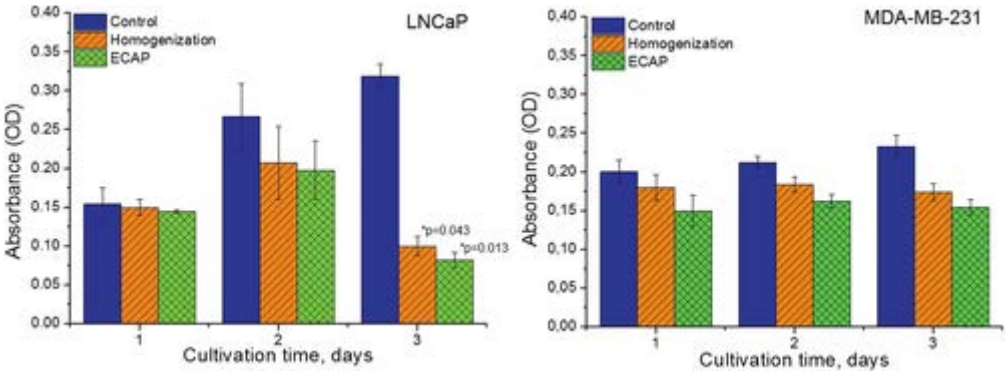

Figure 2
MTT assay results on cell proliferation in terms of the absorbance values after 1–3 days incubation with the alloy (left: LNCaP, right: MDA-MB-231; mean ± SD, *$p < 0.05$).

Compared with the control, MDA-MB-231 cell proliferation on the ECAP-processed samples after day 2 and day 3 was reduced by a factor of 1.3 and 1.5, respectively. For samples of the alloy in the initial homogenized condition (Hom.), a verifiable effect was detected only after day 3, the number of living cells being reduced by a factor of 1.3 as compared with the control.

Based on these results, it can be stated with confidence that ECAP-treated alloy WE43 was more efficient as an antitumor agent than the homogenized one.

Degradation rate

The tests conducted showed that the rate of biodegradation of WE43 samples in both microstructural states was close: 0.96 ± 0.51 mm/year in the homogenized and 1.57 ± 0.19 mm/year in the ECAP-processed condition (Fig. 3). This rate is a good compromise between a typically desirable DR in bone implantology, which should be around 1 mm/year or less and antitumor activity. The observed acceleration of biodegradation by ECAP processing, while suggesting a qualitative trend, cannot be considered as statistically relevant, though (*$p > 0.05$).

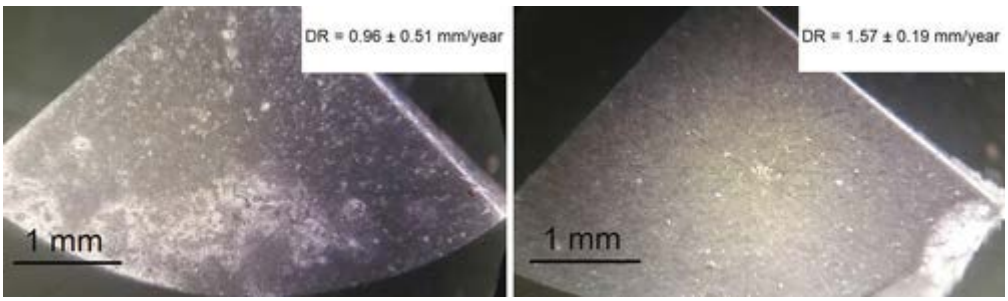

Figure 3
Specimen surface before removal of the corrosion products of the WE43 alloy in (a) homogenized and (b) ECAP-treated state after incubation in RPMI-1640 medium for 3 days (DR stands for DR).

Induction of apoptosis

Investigation of the mechanism of cell death has shown that contact with the alloy causes the induction of apoptosis of both tumor cell lines (Fig. 4). Again, the effect of WE43 was more pronounced for the ECAP-processed samples.

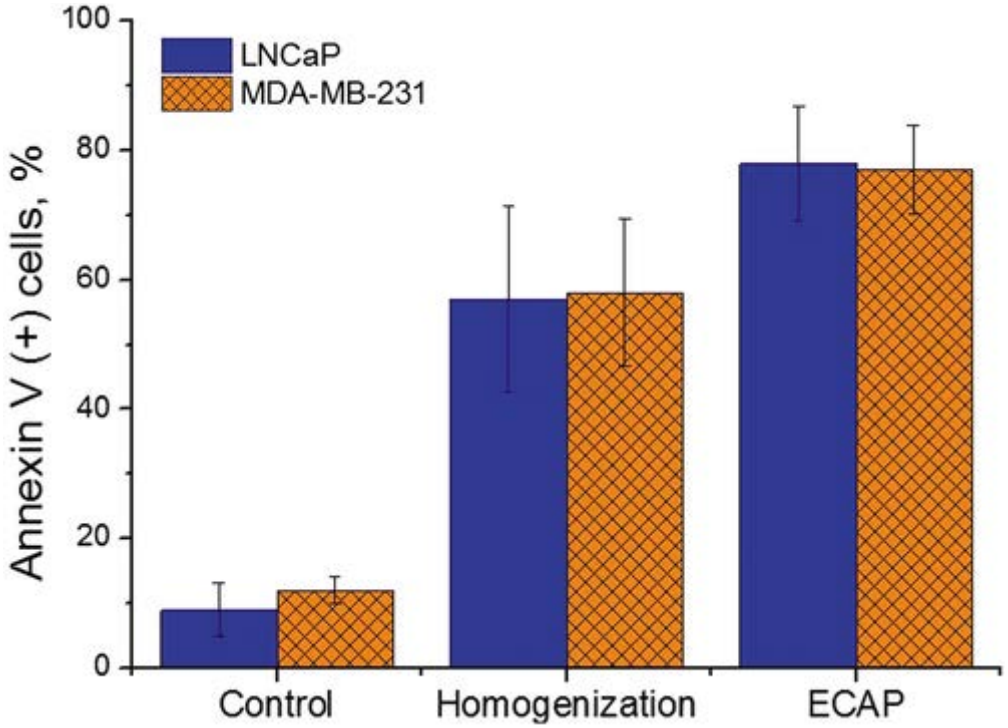

Figure 4
Induction of LNCaP and MDA-MB-231 tumor cells apoptosis as a result of 3-day coincubation with samples of the WE43 alloy in homogenized and deformed states. Mean ± SD, **p* < 0.05.

Oxidative stress

Coincubation of homogenized or ECAP-modified alloy with LNCaP and MDA-MB-231 tumor cells led to a decrease in the amount of oxygen radicals expressing the concentration of ROS(+) cells (Fig. 5). This trend was statistically verified for LNCaP cells over day 1 to day 3, and for MDA-MB-231 cells on the third day of cultivation.

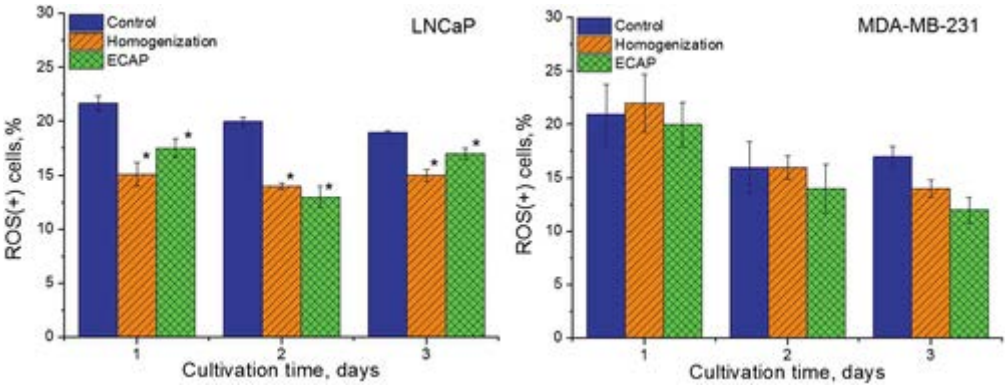

Figure 5
Effect of the WE43 alloy in homogenized and ECAP-treated states on the change in ROS(+) cells concentration after coincubation with LNCaP (left) or MDA-MB-231 (right) tumor cells in vitro. Mean ± SD, *$p < 0.05$.

Bcl-2(+) tumor cells concentration

Figure 6 shows a significant decrease in the concentration of Bcl-2 (+) cells during the incubation of LNCaP tumor cells with the samples of both states of the alloy—by 9–14% compared with the control.

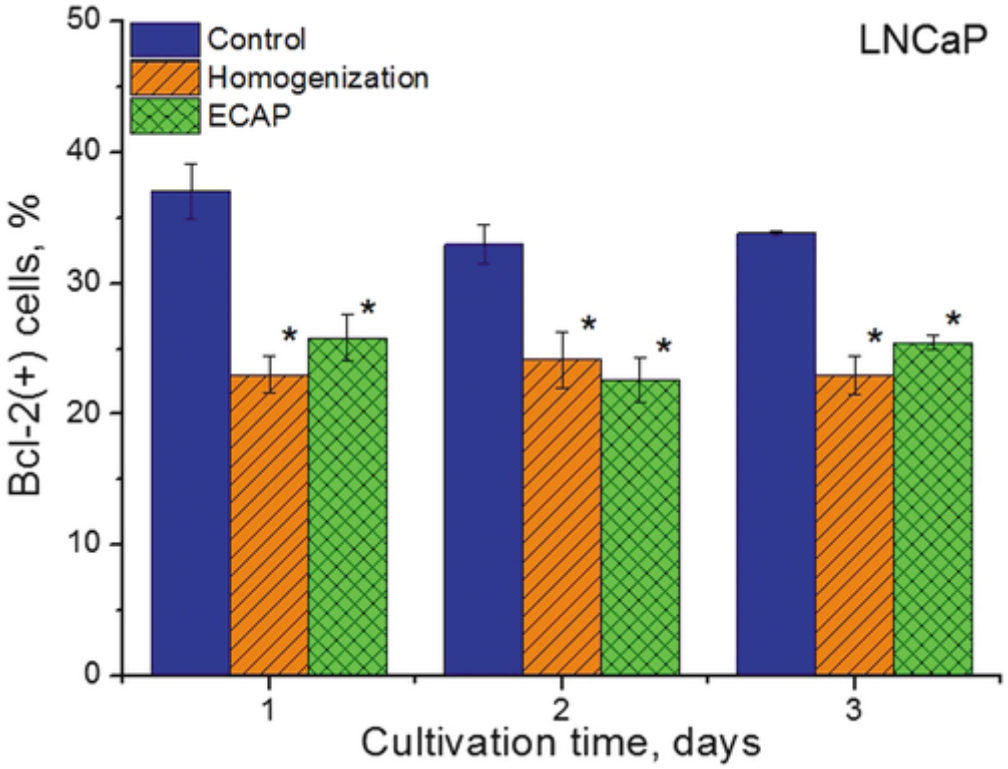

Figure 6
Influence of the WE43 alloy in homogenized and ECAP-treated states on the concentration of Bcl-2(+) LNCaP tumor cells. Mean ± SD, *$p < 0.05$.

DISCUSSION

In this study, the antitumor activity of alloy WE43 with respect to the human breast tumor cell line MDA-MB-231 and the human prostate tumor cell line LNCaP was investigated. These tumors are characterized by a frequent occurrence of bone metastasis, so that these cell lines could be regarded as relevant models for the study of the material, which is primarily intended for orthopedic oncology.

Two variants of the WE43 alloy, homogenized and ECAP-treated one, were investigated. The data obtained showed that both WE43 variants of the alloy had a cytotoxic effect on tumor cells *in vitro*. The ECAP-treated version turned out to be more effective than its homogenized counterpart.

The observed cytotoxic activity can be correlated with several factors. A relatively fast degradation of the material will enhance the release of RE elements, thus supporting the

anticancerous activity, which is consistent with the previously reported data on the same properties of the EW62 alloy (Mg–6%Nd–2%Y–0.5%Zr).[14] In addition, the observed cytotoxic effect may be a result of the biodegradation-induced rise of the pH level of the culture medium, which is damaging to tumor cells because of the osmotic shock they experience. Overall, the corrosion rate of alloy WE43 in the initial and ECAP-modified conditions is hardly distinguishable statistically. However, within the measurement error, the corrosion rate of the ECAP-modified alloy was somewhat higher (0.96 ± 0.51 mm/year in the homogenized and 1.57 ± 0.19 mm/year in the ECAP-processed condition). Several factors are seen to be responsible for the corrosion behavior of magnesium alloys with Ultrafine grained (UFG) structure.[20] On the one hand, grain refinement leads to an increase in the total grain boundary area and, accordingly, the length of grain boundaries facing the sample surface. This gives rise to acceleration of corrosion, as grain boundaries possess an excess energy over the bulk. On the other hand, the formation of the UFG structure was shown to lead to a decrease in the surface roughness—an effect that decelerates corrosion.[21] This effect counteracts that of the increased grain boundary area. The interplay of the various surface phenomena that may be influenced by severe plastic deformation (SPD) processing (including wettability, surface charge variation, texture development, etc.) with the mentioned ones may lead to both an increase and decrease in the resultant corrosion rate. Which of the two opposite trends prevails depends on the alloy system and the thermomechanical process the material has undergone.[22, 23] It should also be kept in mind that in the alloy under consideration here, ECAP processing leads to precipitation of RE-rich $Mg_{41}Nd_5$ particles, which exhibits a lower corrosion rate than the Mg matrix. Our tentative conclusion is that in our case the entirety of the possible phenomena is balanced, the net effect of ECAP on the overall corrosion rate being small, yet discernible. We also note that the high RE content of the $Mg_{41}Nd_5$ phase may produce an additional cytotoxic effect on tumor cells when the $Mg_{41}Nd_5$ particles degrade. Hence, the greater antitumor activity of ECAP-processed WE43 may be associated with the grain refinement this process produces, while also causing precipitation of the RE-enriched phase $Mg_{41}Nd_5$.

Our study has established that the tumor cell death caused by the contact with the samples of the alloy was due to the induction of apoptosis. Similar conclusions were drawn in a study of the mechanism of cell death during incubation with other magnesium alloys.[24] By employing phenotype Annexin V(+) PI(−) cells, we demonstrated that after 2–3 days of incubation with WE43, a significant part of the tumor cells, while still retaining signs of viability, was at an early stage of apoptosis. With an increase of the incubation time, the percentage of Annexin V(+) PI(+) cells increased, indicating the occurrence of late apoptosis. As mentioned above, the development of apoptosis in cells under the influence of metal ions can be due to a change in the mitochondrial membrane potential, activation of the caspase cycle, and suppression of MAPK activation.[10] In addition, among the main triggers of cell apoptosis include oxidative stress.[25] The formation of free radicals of oxygen is ubiquitous in biological systems and is a direct result of specific enzymatic processes. It is also associated with a side process of oxidation–reduction reactions in a cell. A decrease in the concentration of ROS can lead to a shift in the redox potential of the mitochondrial respiratory chain carriers responsible for the synthesis of ATP and determining the energy potential of the cell.[26] Previously, it was found that in the process of biodegradation of the WE43 alloy, hydrogen evolution occurs,[27] which may have an effect on the redox potential, which was shown in the present study; during the incubation of tumor cells with WE43 alloy, release of the oxygen radicals (ROS) by the cells was diminished. Consequently, oxidative stress in the incubation of tumor cells with WE43 can be ruled out as a cause of the induction of apoptosis. Rather, apoptosis of the tumor cells studied can be associated with the release of RE elements or hydrogen ions during the

biodegradation of WE43, which leads to an increase in the pH value of the medium during coincubation of this alloy with the cells.[28]

Bcl-2 is another significant factor involved in the development of apoptosis. It is generally believed that the cell inhibits the initiation of apoptosis due to the production of this protein and its subsequent phosphorylation.[26] In the present study, it was found that the concentration of Bcl-2 (+) tumor cells was significantly reduced in the presence of the alloy. Probably, this phenomenon is associated with a decrease in the protein-synthesizing function of the cell, in general, due to the lack of ATP caused by a change in the membrane potential and inhibition of the mitochondria respiratory chain function. As an alternative mechanism, the initiation of apoptosis in tumor cells may be mediated by caspases or apoptotic protease activating factor whose activity was downregulated by Bcl-2.[29]

It should be noted that despite the daily renewal of the growth medium, a tendency to nonuniform reduction of the viability and proliferation activity of tumor cells coincubated with the samples of the alloy was observed. A possible reason is an increase in the contact area with the incubation medium due to growing erosion of the sample surface and the concomitant increase of the release of the toxic constituents of the alloy (ions of Mg and REs, OH^-, etc.). Besides, the contact with the alloy may trigger a cascade of reactions of apoptosis in the cell population owing to the release of signaling molecules from dying cells through paracrine signaling.[30] These mechanisms may explain the observed progressive nonspecific inhibition of cell viability and proliferation. Given a fairly low rate of biodegradation of the alloy considered limiting the release of cytotoxic agents into the growth medium, this explanation appears plausible. In this case, the occurrence of bioactive degradation products (such as Mg and RE-ions, OH-, or others), even in a small concentration, at an early stage of incubation may efficiently trigger apoptosis of tumor cells, thus inhibiting their proliferation and causing their death. Hence, the data obtained, along with the available scarce information about the effect of magnesium alloys on the viability of tumor cells, lead to the conclusion that alloying of Mg with various elements, including REs, provides it with a nonspecific cytotoxicity to malignantly transformed cells.

According to our data presented above, alloy WE43 reduced the viability of the LNCaP and MDA-MB-231 cells by 21 and 31%, respectively. A natural question here is whether the observed cytotoxic effects owe to the presence of the RE elements in the alloy or are due to the base material—magnesium itself. There is currently no full consensus on this issue. Thus, Charyeva et al.[31] demonstrated that alloy WE43 as well as Mg10Gd impaired cell viability more than pure magnesium did. However, other studies did not confirm that of RE elements, which can be identified as the principal agent causing cytotoxicity.[32] Further studies are needed to determine whether magnesium is a sole factor causing cytotoxicity, or just provides a “background” to that of the RE elements in alloy WE43 or, possibly, acts in concert with them. Whatever the root cause of the effect may be, the present results demonstrate unequivocally that alloy WE43 does show an inhibitive action on tumor cells.

It should be noted that the effects observed, as unquestionable as they are, cannot be regarded as fully sufficient for therapeutic use. It may thus be suggested that to employ the alloys in implants with antitumor activity, further cytotoxic components, such as substances used in the chemotherapy of cancer patients, need to be added to Mg alloys. In that case, gradual bioresorption of the alloy would give rise to a preprogrammed release of the cytostatic with an efficient local concentration not causing systemic side effects.

We also note that the applicability of *in vitro* results for alloy WE43 reported here to the *in vivo* conditions is not warranted because of a much greater buffering capacity of the *in vivo* environment. This was demonstrated by Brooks et al.[33] for *Acinetobacter baumannii* (Ab307) bacteria cultured on AZ91 samples. Similarly, biocorrosion of alloy WE43 was shown[34] to be much slower under *in vivo* than *in vitro* conditions. Thus, the present results should not prejudice the outcomes of future *in vivo* studies on the response of tumor cells to alloy WE43 in various microstructural states.

CONCLUSION

The data presented suggest that alloy WE43 with an optimal DR can be considered as a promising material with antitumor activity for implants and fasteners for orthopedic oncology. It was found that the ECAP treatment of the alloy, along with the known improvement of mechanical properties, leads to an increase in the cytotoxic activity against tumor cells. While the intensity of the antitumor activity of the alloy cannot be considered sufficient for achieving the desired levels of antiproliferative effect, the very occurrence of such an effect demonstrated by the present study may open interesting avenues for orthopedic oncology. Therefore, we deem it appropriate to continue work on developing alloys for implants with local tumor activity by ligating magnesium alloys with bioactive elements, such as REs, or by introducing cytotoxic/cytostatic compounds into their composition. Mechanical processing of the alloys by SPD, such as ECAP, offers an additional possibility of obtaining Mg-based implants with superior strength and enhanced antitumor activity.

ACKNOWLEDGMENTS

This research was funded through RSF grant #18-45-06010 and HRSF grant #LK11101WBP0303. Our thanks go to Dr. G. Gerstein who supplied the WE43 castings used in this work. The expert assistance of Dr. G. I. Raab with ECAP processing is gratefully acknowledged.

REFERENCES

1. Peng QM, Li XJ, Ma N, Liu R, Zhang H. Effects of backward extrusion on mechanical and degradation properties of Mg-Zn biomaterial. J Mech Behav Biomed 2012;10:128–137. https://doi.org/10.1016/j.jmbbm.2012.02.024.

2. Li Y, Liu GW, Zhai ZJ, Liu L, Li H, Yang K, Tan L, Wan P, Liu X, Ouyang Z, Yu Z, Tang T, Zhu Z, Qu X, Dai K. Antibacterial properties of magnesium in vitro and in an in vivo model of implantassociated

methicillin-resistant Staphylococcus aureus infection. Antimicrob Agents Chemother 2014;58:7586–7591. https://doi.org/ 10.1128/AAC.03936-14.

3. Li M, Ren L, Li LH, He P, Lan GB, Zhang Y, Yang K. Cytotoxic effect on osteosarcoma MG-63 cells by degradation of magnesium. J Mater Sci Technol 2014;30:888–893. https://doi.org/10.1016/j.jmst.2014.04.010.

4. Chen J, Tan L, Yu X, Etim IP, Ibrahim M, Yang K. Mechanical properties of magnesium alloys for medical application: A review. J Mech Behav Biomed Mater 2018;87:68–79. https://doi.org/10.1016/ j.jmbbm.2018.07.022.

5. Kim J, Gilbert JL. In vitro cytotoxicity of galvanically coupled magnesium-titanium particles on human osteosarcoma SAOS2 cells: A potential cancer therapy. J Biomed Mater Res B Appl Biomater 2019;107(1):178–189. https://doi.org/10.1002/jbm.b.34109.

6. Kim J, Gilbert JL. The effect of cell density, proximity, and time on the cytotoxicity of magnesium and galvanically coupled magnesium– titanium particles in vitro. J Biomed Mater Res A 2018;106(5):1428–1439. https://doi.org/10.1002/jbm.a.36334.

7. Chen YM, Xiao M, Zhao H, Yang B. On the antitumor properties of biomedical magnesium metal. J Mater Chem B 2015;3:849–858. https://doi.org/10.1039/C4TB01421A.

8. Wu Y, He G, Zhang Y, Liu Y, Li M, Wang X, Li N, Li K, Zheng G, Zheng Y, Yin Q. Unique antitumor property of the Mg-Ca-Sr alloys with addition of Zn. Sci Rep 2016;6:21736. https://doi.org/10.1038/srep21736.

9. Fazel Anvari-Yazdi A, Tahermanesh K, Hadavi SM, et al. Cytotoxicity assessment of adipose-derived mesenchymal stem cells on synthesized biodegradable Mg-Zn-Ca alloys. Mater Sci Eng C Mater Biol Appl 2016;69:584–597. https://doi.org/10.1016/j.msec.2016.07.016.

10. Puvvada N, Rajput S, Prashanth Kumar BN, et al. Novel ZnO hollow-nanocarriers containing paclitaxel targeting folate-receptors in a malignant pH-microenvironment for effective monitoring and promoting breast tumor regression. Sci Rep 2015;5(11760). https://doi.org/10.1038/srep11760.

11. Wang XP, Li X, Onuma K, Sogo Y, Ohno T, Ito A. Zn- and Mgcontainingtricalcium phosphates-based adjuvants for cancer immunotherapy. Sci Rep 2013;3(2203). https://doi.org/10.1038/ srep02203.6

12. Meyer K, Rajanahalli P, Ahamed M, Rowe JJ, Hong Y. ZnO nanoparticles induce apoptosis in human dermal fibroblasts via p53 and p38 pathways. Toxicol In Vitro 2011;25:1721–1726. https://

doi.org/10.1016/j.tiv.2011.08.011.

13. Fischer J, Pröfrock D, Hort N, Willumeit R, Feyerabend F. Improved cytotoxicity testing of magnesium materials. Mat Sci Eng B 2011; 176:830–834. https://doi.org/10.1016/j.mseb.2011.04.008.

14. Hakimi O, Ventura Y, Goldman J, Vago R, Aghion E. Porous biodegradable EW62 medical implants resist tumor cell growth. Mater Sci Eng C Mater Biol Appl 2016;61:516–525. https://doi.org/10.1016/ j.msec.2015.12.043.

15. Windhagen H, Radtke K, Weizbauer A, Diekmann J, Noll Y, Kreimeyer U, Schavan R, Stukenborg-Colsman C, Waizy H. Biodegradable magnesium-based screw clinically equivalent to titanium screw in hallux valgus surgery: Short term results of the first prospective, randomized, controlled clinical pilot study. Biomed Eng Online 2013;12:62. https://doi.org/10.1186/1475-925X-12-62.

16. Witte F, Kaese V, Haferkamp H, Switzer E, Meyer-Lindenberg A, Wirth CJ, Windhagen H. In vivo corrosion of fourmagnesium alloys and the associated bone response. Biomaterials 2005;26:3557–3563. https://doi.org/10.1016/j.biomaterials.2004.09.049.

17. Estrin Y, Vinogradov A. Extreme grain refinement by severe plastic deformation – A wealth of challenging science. Acta Mater 2013;61 (3):782–817. https://doi.org/10.1016/j.actamat.2012.10.038.

18. Valiev RZ, Islamgaliev RK, Alexandrov IV. Bulk nanostructured materials from severe plastic deformation. Prog Mater Sci 2000;45: 103–189. https://doi.org/10.1016/S0079-6425(99)00007-9.

19. Martynenko NS, Lukyanova EA, Serebryany VN, Gorshenkov MV, Shchetinin IV, Raab GI, Dobatkin SV, Estrin Y. Increasing strength and ductility of magnesium alloy WE43 by equal-channel angular pressing. Mater Sci Eng A 2018;712:625–629. https://doi.org/10.1016/j.msea.2017.12.026.

20. Ahmadkhaniha D, Fedel M, Heydarzadeh SM, et al. Corrosion behavior of severely plastic deformed magnesium based alloys: A review. Surf Eng Appl Electrochem 2017;53(5):439–448.

21. Medvedev AE, Neumann A, Ng HP, et al. Combined effect of grain refinement and surface modification of pure titanium on the attachment of mesenchymal stem cells and osteoblast-like SaOS-2 cells. Mater Sci Eng C 2017;71:746–757.

22. Op't Hoog C, Birbilis N, Zhang M-X, Estrin Y. Surface grain size effects on the corrosion of magnesium. Key Eng Mater 2008;384: 229–240. https://doi.org/10.4028/www.scientific.net/KEM.384.229.

23. Op't Hoog C, Birbilis N, Estrin Y. Corrosion of pure Mg as a function of grain size and processing route. Adv Eng Mater 2008;10(6): 579–582. https://doi.org/10.1002/adem.200800046.

24. Li M, Wang W, Zhu Y, Lu Y, Wan P, Yang K, Zhang Y, Mao C.Molecular and cellular mechanisms for zoledronic acid-loaded magnesiumstrontium alloys to inhibit giant cell tumors of bone. Acta Biomater 2018;77:365–379. https://doi.org/10.1016/j.actbio.2018.07.028.

25. Kannan K, Jain SK. Oxidative stress and apoptosis. Pathophysiology 2000;7(3):153–163. https://doi.org/10.1016/S0928-4680(00)00053-5. 26. Tök L, Nazıro_glu M, U_guz AC, Tök Ö. Elevated hydrostatic pressures induce apoptosis and oxidative stress through mitochondrial membrane depolarization in PC12 neuronal cells: A cell culture model of glaucoma. J Recept Signal Transduct Res 2014;34(5):410–416. https://doi.org/10.3109/10799893.2014.910812.

27. Dobatkin SV, Lukyanova EA, Martynenko NS, Anisimova NY, KiselevskiyMV, GorshenkovMV, Yurchenko NY, Raab GI, Yusupov VS, Birbilis N, Salishchev GA, Estrin YZ. Strength, corrosion resistance, and biocompatibility of ultrafine-grained Mg alloys after different modes of severe plastic deformation. IOP Conf Ser Mater Sci 2017;194:012004. https://doi.org/10.1088/1757-899X/194/1/012004.

28. Kale J, Osterlund EJ, Andrews DW. BCL-2 family proteins: Changing partners in the dance towards death. Cell Death Differ 2018;25:65–80. https://doi.org/10.1038/cdd.2017.186.

29. Yuan Y, Wu J, Li B, Niu J, Tan H, Qiu S. Regulation of signaling pathways involved in the anti-proliferative and apoptosis-inducing effects of M22 against non-small cell lung adenocarcinoma A549. Sci Rep 2018;8(1):992. https://doi.org/10.1038/s41598-018-19368-0.

30. Boland K, Flanagan L, Prehn JHM. Paracrine control of tissue regeneration and cell proliferation by Caspase-3. Cell Death Dis 2013;4(7): e725. https://doi.org/10.1038/cddis.2013.250.

31. Charyeva O, Dakischew O, Sommer U, Heiss C, Schnettler R, Lips KS. Biocompatibility of magnesium implants in primary human reaming debris-derived cells stem cells in vitro. J Orthop Traumatol 2015;17: 63–73. https://doi.org/10.1007/s10195-015-0364-9.

32. Yang L, Hort N, Laipple D, Höche D, Huang Y, Kainer KU, Willumeit R, Feyerabend F. Element distribution in the corrosion layer and cytotoxicity of alloy Mg-10Dy during in vitro biodegradation. Acta Biomater 2013;9(10):8475–8487. https://doi.org/10.1016/j.actbio.2012.10.001.

33. Brooks EK, Ahn R, Tobias ME, Hansen LA, Luke-Marshall NR, Wild L, Campagnari AA, Ehrensberger MT. Magnesium alloy AZ91 exhibits antimicrobial properties in vitro but not in vivo. J Biomed Mater Res B Appl Biomater 2018;106(1):221–227. https://doi.org/10.1002/jbm.b.33839.

34. Lukyanova E, Anisimova N, Martynenko N, Kiselevsky M, Dobatkin S, Estrin Y. Features of in vitro and in vivo behaviour of magnesium alloy WE43. Mater Lett 2018;215:308–311. https://doi.org/10.1016/j.matlet.2017.12.125.